Journal of Zhejiang University-SCIENCE A
www.jzus.zju.edu.cn; www.springer.com/journal/11582
E-mail: jzus_a@zju.edu.cn

Research Article
https://doi.org/10.1631/jzus.A2500239

Impact of heterogeneous electrode design on vanadium redox flow batteries with different flow fields

Jie SUN[1], Menglian ZHENG[2,3]✉, Mengxin YU[1], Jinbo CHEN[1], Jianxin LI[1], Changxing HU[1]

[1]*Institute of Energy and Environment Engineering, NingboTech University, Ningbo 315100, China*
[2]*Institute of Thermal Science and Power Systems, College of Energy Engineering, Zhejiang University, Hangzhou 310027, China*
[3]*State Key Laboratory of Clean Energy Utilization, Hangzhou 310027, China*

Abstract: With the rapid progress of processing technology, the heterogeneous optimization design of porous electrodes is becoming practicable. Nevertheless, there is currently a lack of understanding of the relevant theoretical foundation. In this study, we systematically examine the influence and mechanism of various carbon paper (CP) stacking schemes on the performance of vanadium redox flow batteries (VRFBs) with different flow fields (interdigitated flow field, IFF, and serpentine flow field, SFF) through experiments and simulations. We find that the optimization of porous electrode heterogenization shows significant differences. For the IFF, optimizing the porous electrode structure remarkably improves the mass transfer effect near the membrane, thus enhancing the performance of VRFBs. For the SFF, the effectiveness of electrode structure optimization is manifested mainly in the improvement of the permeability of the porous electrode. Furthermore, the effectiveness of the heterogeneous design of the porous electrode depends on a balanced relationship between the mass transfer rate of the reactants and the rate of the electrochemical reaction. The Damköhler number is introduced to measure this balance and serve as a basis for subsequent optimization.

Key words: Vanadium redox flow battery (VRFB); Serpentine flow field (SFF); Interdigitated flow field (IFF); Heterogeneous electrode design; Carbon paper (CP); Damköhler number

1 Introduction

Vanadium redox flow batteries (VRFBs) represent a promising electrochemical energy storage technology due to their long cycle life, quick response, high reliability, and absence of electrolyte cross-contamination (Gautam and Kumar, 2022; Ye JY et al., 2024; Ye LZ et al., 2024). To promote the large-scale industrialization of VRFBs, research has focused on improving their power density to reduce system costs (Huang et al., 2022a; Zarei-Jelyani et al., 2023; Huynh et al., 2025). The porous electrode, which not only provides active sites for redox reactions but also affects the ion and mass transport within it, plays a crucial role in reducing the high polarization in VRFBs (He et al., 2022; Wang et al., 2024). In addition to using various pretreatment methods to improve the surface activity of the porous electrode (Ye et al., 2022), enhancing its structural design can optimize its performance (Forner-Cuenca and Brushett, 2019; Ye LZ et al., 2024). Since changes in the pore structure of the electrode can lead to alterations in the specific surface area, structural optimization often results in the coupled refinement of its mass transfer and electrochemical processes (Lv et al., 2024).

Electrode structure optimization can generally be either homogeneous or heterogeneous. This classification is based on whether there is overall consistency or local differences in the porous structure of the electrode (Wan et al., 2021; Alphonse et al., 2023). Given that the electrochemical reaction occurs nonlinearly in the electrode and that reactants are non-uniformly distributed from the inlet to the outlet, heterogeneous optimization is more intricate. It often produces better results in balancing the mass transfer property and specific surface area. For instance, Hu et al. (2018) reported a hybrid electrode composed of graphene

✉ Menglian ZHENG, menglian_zheng@zju.edu.cn
Menglian ZHENG, https://orcid.org/0000-0002-4418-4361

Received June 8, 2025; Revision accepted Oct. 22, 2025;
Crosschecked Mar. 26, 2026

© Zhejiang University Press 2026

oxide for enhanced reactivity and reduced graphene foam for improved conductivity. This electrode significantly reduces battery polarization, thereby enhancing the charge and discharge capacity and efficiency. Jiang et al. (2019a, 2019b) and Chen et al. (2019) proposed novel electrode structures with gradient or double-layered porous media from the bipolar plate side to the membrane side. These structures aim to balance the requirements of sufficient mass transport and a high specific surface area in the flow cell, resulting in a lower charge voltage and a higher discharge voltage for VRFBs. Research by Yoon et al. (2019) showed that optimizing the porosity distribution in the in-plane direction of the porous electrode to match the reactant concentration distribution is crucial for increasing the power density and energy efficiency of the flow cell without a flow field design. Thus, carrying out heterogeneous and sophisticated optimization design on porous electrodes is an effective approach to enhance the power density of VRFBs.

The non-uniform distribution of reactant transfer and electrochemical reactions within the porous electrode provides a practical foundation and rationale for its heterogeneous optimization design (Mukhopadhyay et al., 2019; Zeng et al., 2023). This non-uniform distribution is closely associated with the flow field structure, which is an essential factor that should not be overlooked during the optimization process (Huang et al., 2022a, 2022b). For example, Pezeshki et al. (2017) and Maurya et al. (2018) both discovered that the performance of flow cells using different electrode materials is closely related to the type of flow fields. In the case of a flow cell with a serpentine flow field (SFF), the mass transfer overpotential in carbon paper (CP) electrodes is significantly higher than that of carbon felt (Duan et al., 2022; Wang et al., 2022). However, for a flow cell with equal path length (EPL) flow fields, this drawback has been eliminated (Houser et al., 2017). Houser et al. (2016) found that increasing the number of layers of CP electrodes can significantly reduce the mass transfer overpotential of the flow cell with SFF. In contrast, for a flow cell with an interdigitated flow field (IFF), the influence of the number of layers of CP is not significant. Therefore, we conclude that during the optimization design process of porous electrodes, the influence of flow fields should be fully considered (Muñoz-Perales et al., 2023).

CP is thin and has a high specific surface area. Its stacked use was first proposed in the zero-gap design (Maurya et al., 2018). Previous studies have shown that this method can significantly enhance the power density and energy efficiency of VRFBs. However, the underlying basis of its enhanced performance still requires in-depth understanding. Although previous research has explored heterogeneous electrodes by layering different numbers and types of CP, it remains unclear how the structure of layered electrodes, in combination with flow field designs, improves the reactant concentration and thereby the overpotential distribution. Therefore, in this study, we aim to address the question of how to conduct heterogeneous optimization design of porous electrodes for flow cells implemented with different flow fields. Given their extensive applications, we focus on two types of flow fields: IFF and SFF. Moreover, based on our previous findings, the non-uniformity of mass transfer and electrochemical reactions occurs mainly in the through-plane direction of the electrode under these two flow fields (Sun et al., 2019b). Thus, we focus mainly on the heterogeneous optimization design of the porous electrode in this direction. Two representative CP electrodes (SGL39AA and SGL38AA) are combined to form a single electrode for heterogeneous design.

The remainder of this paper is structured as follows. Section 2 details the design of the heterogeneous electrode for the flow cell. Section 3 describes the experimental and simulation methods used in this study. In Section 4, we present and discuss the experimental and simulation results of different heterogeneous electrode designs for VRFBs implemented with different flow fields. Finally, Section 5 presents the conclusions and future research directions.

2 Approaches

2.1 Combined electrode design for VRFBs with IFF or SFF

Two different CPs (SGL39AA and SGL38AA) were used. Their typical physical properties (Table 1) were supplied by the manufacturer (SGL Carbon Group, Germany) or experimentally determined. The pore diameter of SGL39AA (42–44 μm) is larger than that of SGL38AA (25–29 μm); therefore, its porosity

Table 1 Typical properties of SGL39AA and SGL38AA

Typical property	Description	
	SGL39AA	SGL38AA
Thickness[#] (μm)	280	280
Porosity[*] (%)	81	75
Mean pore diameter[#] (μm)	42–44	25–29
Electric conductivity[#] (S/cm)	5	5
Permeability[#] ($\times10^{-12}$ m^2)	11–12	3–4
Specific surface area[*] (m^{-1})	173000	412000

[*]Experimentally determined; [#]Provided by the manufacturer

(81%) and permeability (11×10^{-12}–12×10^{-12} m^2) are also higher than those of SGL38AA (75% and 3×10^{-12}–4×10^{-12} m^2, respectively), but the corresponding specific surface area of SGL39AA (173000 m^{-1}) is smaller than that of SGL38AA (412000 m^{-1}). Note that a higher specific surface area typically corresponds to smaller and more densely distributed pores within the electrode, which in turn reduces its permeability. Consequently, these two properties show an inverse, trade-off relationship, and the performance of a porous electrode fundamentally depends on the balance between the mass transfer rate of reactants and the rate of electrochemical reactions.

Regardless of whether it is IFF or SFF, the flow paths between adjacent tributaries are U-shaped (Fig. 1) (Sun et al., 2023). The main distinction between IFFs and SFFs lies in their overall structure: in an SFF, the inlet and outlet are directly connected, whereas in an IFF, they are not. This structural difference determines whether the process of electrolyte penetration into the porous electrode is active or passive. Specifically, in an IFF, the electrolyte will fully penetrate the electrode, while in SFF, the amount of electrolyte penetrating the electrode depends on the pressure difference between adjacent flow channels and the flow resistance along the U-shaped flow paths (Sun et al., 2022). Our preliminary research indicated that the electrolyte velocity and reactant concentration are strongly correlated with the flow path. This implies that an optimal heterogeneous optimization design should take the flow path as an important reference. Nevertheless, considering the constraints of practical manufacturing, we carried out heterogeneous optimization only in the thickness direction. The complete electrode consisted of three layers of CP in six different combinations (Fig. 1).

2.2 Experimental methods

2.2.1 VRFB single flow cell system

Our experiments were conducted on a VRFB single flow cell system. In the flow cell, the positive and negative SGL® CP electrodes are separated by a Nafion® 117 membrane, and the bipolar plates machined with the flow field are made from graphite composite material (Beijing Jinglong Special Carbon Industrial Co., Ltd., China). Two peristaltic pumps (L/S 07525-40, Masterflex®, USA) were used to cycle the electrolyte (1.6 mol/L vanadyl sulfate dissolved in 4.0 mol/L sulfuric acid solutions, Dalian BR New Material Co., Ltd., China).

2.2.2 *IR*-corrected polarization curve tests

The polarization curves were taken at 0.5 state of charge (SOC) and different flow rates of 5 and

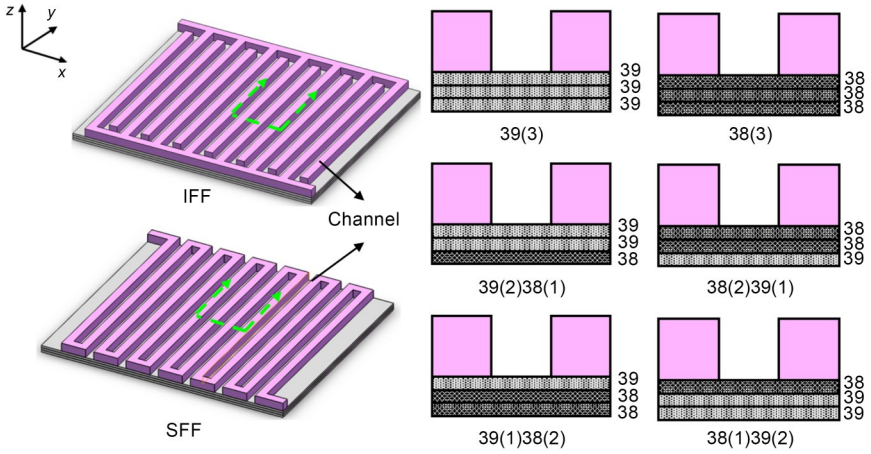


Fig. 1 Combined electrode design for a VRFB with IFF or SFF. They are named according to the top-down order and number of layers

20 mL/min. The two different flow rates represent two distinct operational states in VRFBs: mass transfer-limited and mass transfer-unlimited conditions (see Section 4.2 for a more detailed discussion). To ensure the consistency of SOC during each polarization test, we first used a dedicated VRFB to charge a large volume of electrolyte under constant current conditions for a predetermined duration. The charging duration was determined by charge conservation. Besides, we ensured that the open-circuit equilibrium voltage remained consistent prior to each polarization test. During the measurement, each side used two tanks so that the electrolyte passed through the cell only once without circulation, thereby maintaining a constant electrolyte concentration for the tests. The polarization curves were obtained under potentiostatic control from an open circuit voltage (OCV) of 1.4 to 0.0 V. In addition, the high frequency resistance of the cell was measured under 20 kHz to correct the ohmic loss of the cell for the polarization curves. A Bio-Logic® VSP electrochemical workstation was used for the above tests. Fig. 2 shows the structure of the experimental system.

2.3 Simulation methods

To obtain a more in-depth analysis of how the heterogeneous porous electrode affects the performance of the flow cell, we developed a three-dimensional, multi-physical model with the use of COMSOL Multiphysics®, which can simulate the mass transfer and electrochemical reaction processes in the flow cell. The detailed modeling processes (including geometry, governing equations, boundary conditions, initial values, relevant parameters for the specific battery configuration, and the numerical method) have been published (Sun et al., 2019a). The model used in this study used different CP electrodes, as described in Section 2.1, and was validated in Section S1 of the electronic supplementary materials (ESM).

3 Results

3.1 Performance of combined electrode for a VRFB with an IFF

First, we conduct experimental tests to examine the impact of using a combination electrode on the polarization performance of a VRFB with an IFF (Fig. 3). When only one layer of CP is used as the electrode, we observed that the performance of SGL38AA is better than that of SGL39AA, achieving an approximately 25% increase in the limiting current density (Fig. 3a). We attribute this mainly to the larger specific surface area of SGL38AA, which facilitates an increase in the volumetric mass transfer rate and a reduction in the overpotential within the porous electrode. When the number of electrode layers increases from one to three, although the performance of the VRFB using either SGL38AA or SGL39AA as electrodes

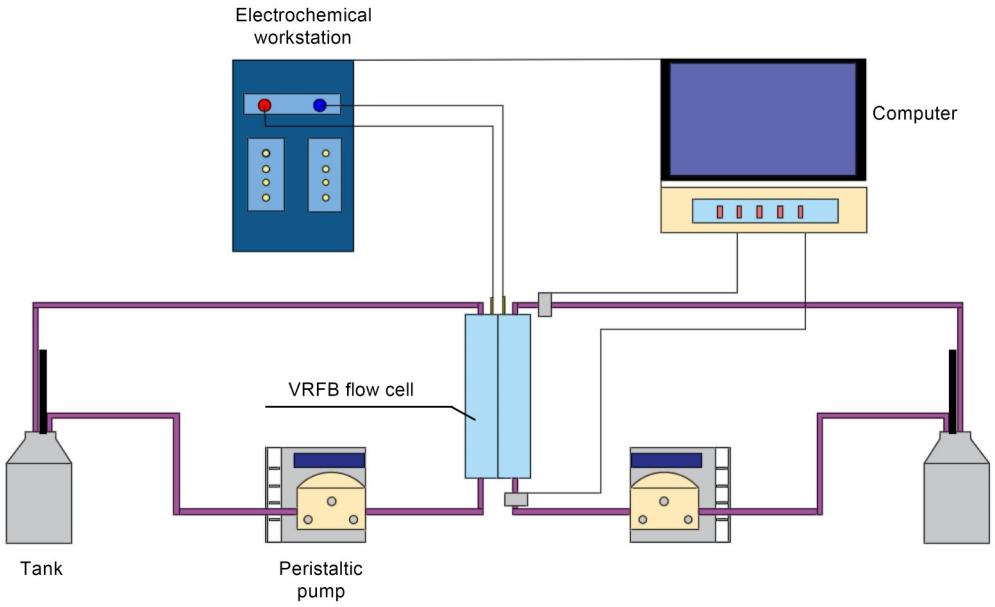


Fig. 2 Experimental system diagram

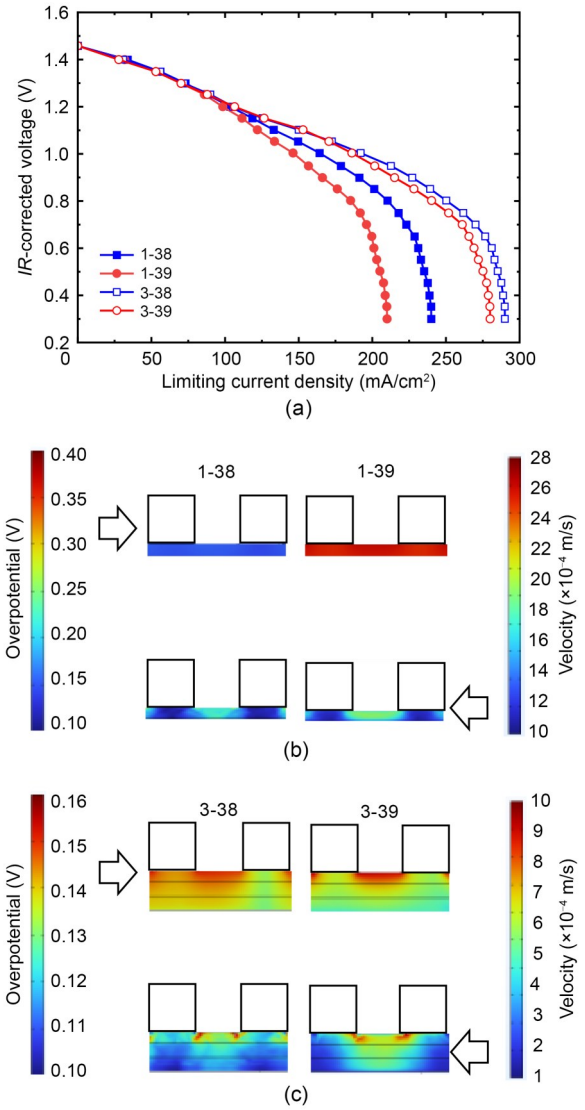


Fig. 3 (a) *IR*-corrected polarization curves of the VRFB flow cell with the IFF and electrodes made of CP with different numbers of layers and types; (b) distribution of overpotential and electrolyte flow velocity in the one-layer CP electrode obtained through simulation; (c) distribution of overpotential and electrolyte flow velocity in the three-layer CP electrode obtained through simulation. Testing was based on a flow rate of 5 mL/min

improves, the increase in the limiting current density achieved by SGL39AA is significantly greater. The limiting current density of the three-layer SGL39AA electrode increases by approximately 50% compared to that of the single-layer SGL39AA electrode, an increase so great that the difference between the two electrodes is negligible in the case of three-layer electrodes. An increase in the number of electrode layers has opposing effects: on the one hand, it enlarges the total reaction area, which is conducive to enhancing the peak current density; on the other hand, the overall increase in electrode thickness leads to a rise in the resistance overpotential. Moreover, the expansion of the overall electrode volume gives rise to more significant unevenness in mass transfer and electrochemical reactions, thereby restricting further improvement of the limiting current density. The enhanced performance of the three-layer SGL39AA is better than that of the three-layer SGL38AA. This indirectly confirms that the unevenness introduced by SGL38AA is more pronounced, which might be associated with the low permeability of SGL38AA, as it impedes the rapid and uniform transfer of ions.

We perform simulations to further elucidate the experimental observations. When there is only one layer of CP electrode, the distribution of the electrolyte flow rate among the two types of CP electrodes is identical (Fig. 3b). Nevertheless, owing to the difference in specific surface area, there is a notable disparity in the overpotential. When the number of electrode layers increases from one to three, the electrolyte flow rate distribution in the electrode composed of SGL39AA is more uniform, thereby avoiding large localized mass transfer overpotentials (Fig. 3c). This compensates for the adverse effect of insufficient specific surface area and is comparable to the overall overpotential of SGL38AA. Consequently, we conclude that in IFF VRFBs, the high permeability of SGL39AA results in low flow resistance, making it more suitable for applications where mass transfer is the limiting factor. In contrast, the high specific surface area of SGL38AA leads to low electrochemical reaction resistance, making it more appropriate for scenarios with favorable mass transfer conditions.

In the porous electrode consisting of three layers of SGL38AA, the poor permeability of SGL38AA causes a lower flow rate of the electrolyte near the membrane side, thereby resulting in poor mass transfer (Fig. 3c). Consequently, we propose replacing the layer of SGL38AA adjacent to the membrane side with SGL39AA while maintaining the other two layers as SGL38AA to leverage its high reactive specific surface area. Thus, the composition of the porous electrode from the bipolar plate side to the membrane side is SGL38AA–SGL38AA–SGL39AA (i.e., higher porosity near the membrane, donated as 38-38-39). Moreover, to demonstrate the effects, we examine the

electrode with the reverse composition (donated as 39-38-38).

We observe that in comparison to the three-layer electrode composed solely of SGL38AA or SGL39AA, the 38-38-39 combination enhanced the limiting current density of the VRFBs by about 17% (Fig. 4a). Conversely, the 39-38-38 combination reduced it by around 20%. Furthermore, according to the simulation results, the efficacy of the 38-38-39 combination stems from two main aspects. First, as mentioned above, the higher permeability of SGL39AA results in reduced flow resistance on the near-membrane side, thereby facilitating a greater distribution of electrolyte to this region. Therefore, positioning SGL39AA on the side adjacent to the membrane significantly enhances mass transfer in the vicinity. Second, placing SGL38AA in a region with superior mass transfer (the side near the bipolar plate) offers sufficient specific surface area for the reaction. These two factors jointly enhance the electrochemical performance of the VRFB. In contrast, for the 39-38-38 combination, SGL38AA exacerbates the deterioration of mass transfer in the near-membrane region. Although SGL39AA increases the electrolyte flow rate near the bipolar plate side, it fails to provide an adequate specific surface area, ultimately leading to a substantial decline in the electrochemical performance of the VRFBs.

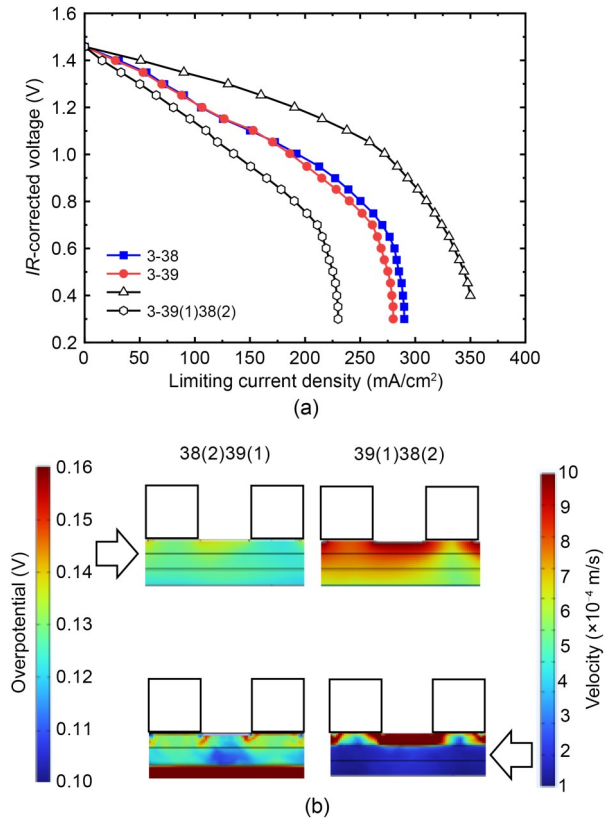


Fig. 4 (a) *IR*-corrected polarization curves of the VRFB flow cell with the IFF and electrodes made of CP with three layers and different combinations; (b) distribution of overpotential and electrolyte flow velocity in the three-layer CP electrode obtained through simulation. Testing was based on a flow rate of 5 mL/min

3.2 Performance of combined electrode for a VRFB with an SFF

Although using the same electrode combination, VRFBs with the SFF or IFF exhibit notable differences in performance. As depicted in Fig. 5a, when the electrode is composed of a single type of CP, regardless of whether it is one or three layers, the performance of the SFF is inferior to that of the IFF. Specifically, the limiting current density of the SFF is generally 20%–60% lower. We attribute this difference to the structural characteristics of the SFF and the resulting fluid dynamics. The SFF features a fully connected flow path from the inlet to the outlet, which implies that the electrolyte may bypass the porous electrode without fully penetrating it before exiting the VRFB. Consequently, the extent of electrolyte penetration into the porous electrode is governed by the flow resistance, or permeability, of the electrode itself. In contrast, the IFF consists of two isolated flow domains, requiring the electrolyte to fully traverse the porous electrode before exiting the system. Therefore, under certain conditions, the degree of electrolyte penetration in SFF VRFBs is necessarily lower than that in IFF VRFBs. Reduced electrolyte penetration typically corresponds to a lower electrolyte velocity within the porous electrode, which ultimately results in reduced polarization performance.

Another aspect worthy of attention is that in VRFBs with the SFF, although SGL38AA has a larger specific surface area, this advantage does not evidently enhance the performance of VRFBs. In contrast, SGL39AA consistently demonstrates better performance. With one layer of CP, SGL39AA leads to an approximately 25% increase in the limiting current density, which rises to approximately 65% when three layers of CP are stacked. The permeability and average pore size of SGL38AA are considerably smaller than those of SGL39AA. This leads to a higher flow resistance, which restricts the penetration of the

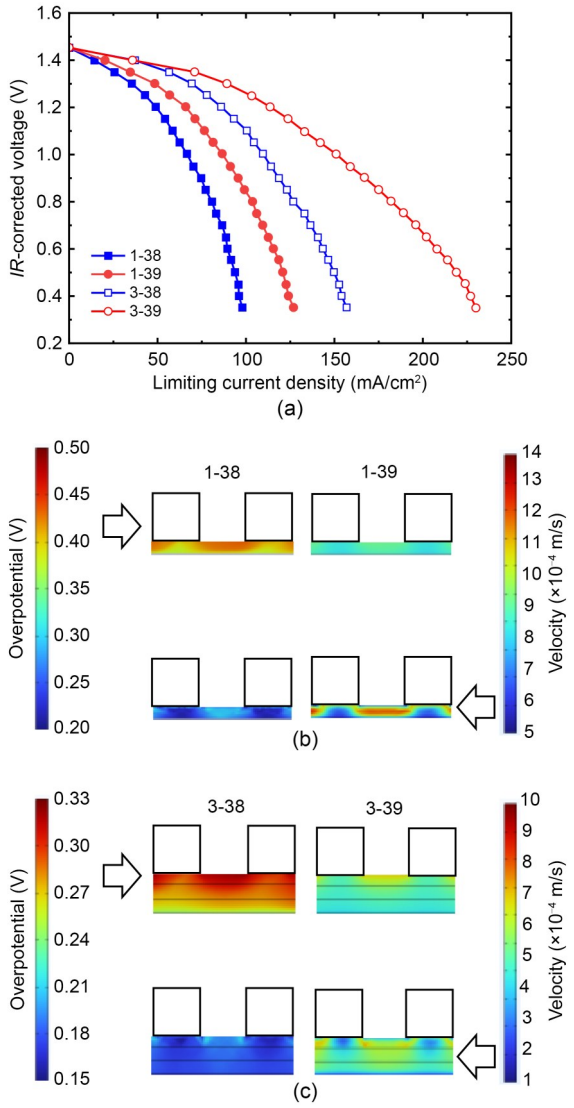


Fig. 5 (a) *IR*-corrected polarization curves of the VRFB flow cell with the SFF and electrodes made of CP with different numbers of layers and types; (b) distribution of overpotential and electrolyte flow velocity in a one-layer CP electrode obtained through simulation; (c) distribution of overpotential and electrolyte flow velocity in the three-layer CP electrode obtained through simulation. Testing was based on a flow rate of 5 mL/min

electrolyte into the porous electrode and ultimately limits the electrochemical performance of the VRFB (details are provided in Table S1 of the ESM). The velocity distributions shown in Figs. 5b and 5c provide a partial explanation for the phenomena. Owing to the limited penetration of the electrolyte, the flow velocity of the electrolyte within the electrode is significantly lower, while the corresponding overpotential loss is substantial. We conclude that for VRFBs with the SFF, the permeability of the porous electrode is a crucial indicator, followed by the specific surface area.

For VRFBs with the SFF, when attempting to use electrodes formed by the combination of SGL38AA and SGL39AA, the resulting effect differs significantly. The performance of the composite electrode is superior to that of the electrode composed solely of SGL38AA (with an approximate 15% increase in the limiting current density) but inferior to that of the electrode composed solely of SGL39AA (with an approximate 25% reduction in the limiting current density) (Fig. 6a). This result aligns with our previous inference. That is, for VRFBs with the SFF, the permeability of the porous electrode is the most crucial factor, followed by the specific surface area of the porous electrode. Whether it is the 39-38-38 combination or the 38-38-39 combination, both contain a layer of SGL39AA electrodes. Therefore, compared to electrodes composed of three layers of SGL38AA, the combined

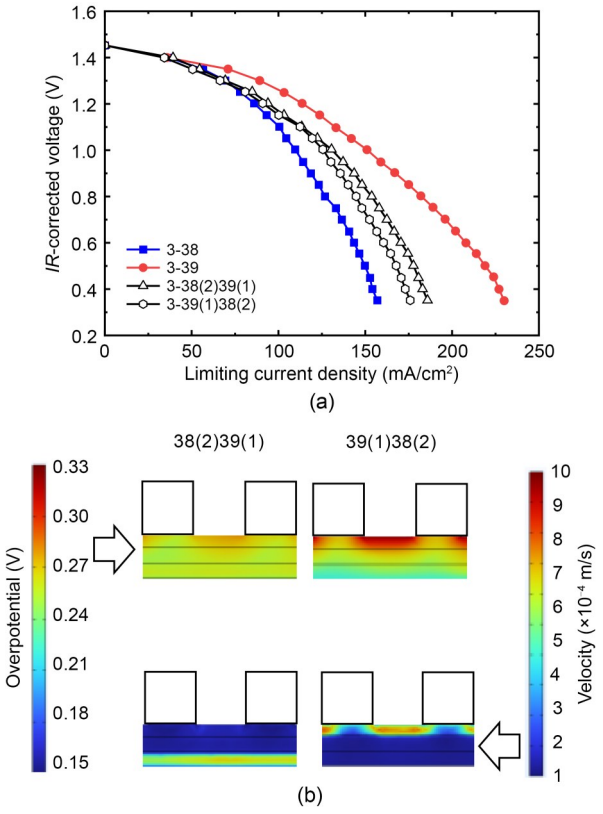


Fig. 6 (a) *IR*-corrected polarization curves of the VRFB flow cell with the SFF and electrodes made of CP with three layers and different combinations; (b) distribution of overpotential and electrolyte flow velocity in the three-layer CP electrode obtained through simulation. Testing was based on a flow rate of 5 mL/min

electrodes achieve a certain degree of enhanced permeability, but they still do not match the performance of electrodes composed of three layers of SGL39AA. Regarding the 38-38-39 combination, its performance is slightly better than that of the 39-38-38 combination, but still falls within the scope of the discussion regarding the complementary advantages of mass transfer and electrochemistry. Specifically, the 38-38-39 combination places the highly permeable SGL39AA in an area with originally poor mass transfer, while the 39-38-38 combination places the SGL39AA with a low specific surface area in an area with originally good mass transfer. Clearly, the distribution strategy of the 38-38-39 combination is better.

4 Discussion

4.1 Dimensionless parameters describing the effectiveness of porous electrodes

The efficacy of this heterogeneous optimization of the porous electrode hinges on the balanced relationship between the mass transfer rate of the reactants and the rate of the electrochemical reaction. We use the Damköhler number (Da^*) to measure this balance and serve as a basis for subsequent optimization.

$$Da^* = \frac{T_{mt}}{T_{rea}} = \frac{k_{rea} a L^2}{k_{mt}}, \tag{1}$$

where T_{mt} is the characteristic time of reactant transport, T_{rea} is the characteristic time of the electrochemical reaction, k_{rea} is the electrochemical reaction rate constant, and k_{mt} is the effective mass transfer coefficient of the diffusion layer (note that during the calculation process, we averaged both k_{rea} and k_{mt} across the entire computational domain. Furthermore, as our previous research (Zheng et al., 2024) indicated that k_{rea} is associated mainly with the modification of the reaction surface and shows minimal correlation with electrode structural parameters or battery operational conditions, it was not explicitly discussed in the subsequent analysis of the results). Moreover, a is the specific surface area of the porous electrode, and L is the characteristic length of reactant transport, which is taken as the thickness of porous electrode. When $Da^* \gg 1$, the system performance is limited by mass transfer. Extensive research has indicated that in VRFBs, the mass transfer process is significantly slower than the electrochemical reaction process and serves as the main limiting factor. Thus, enhancing the material transport process within porous electrodes is of crucial significance. Fig. 7 depicts the electrolyte flow velocity, the effective mass transfer coefficient of the diffusion layer, and the Damköhler number in the porous electrodes of the VRFBs with the IFF or SFF.

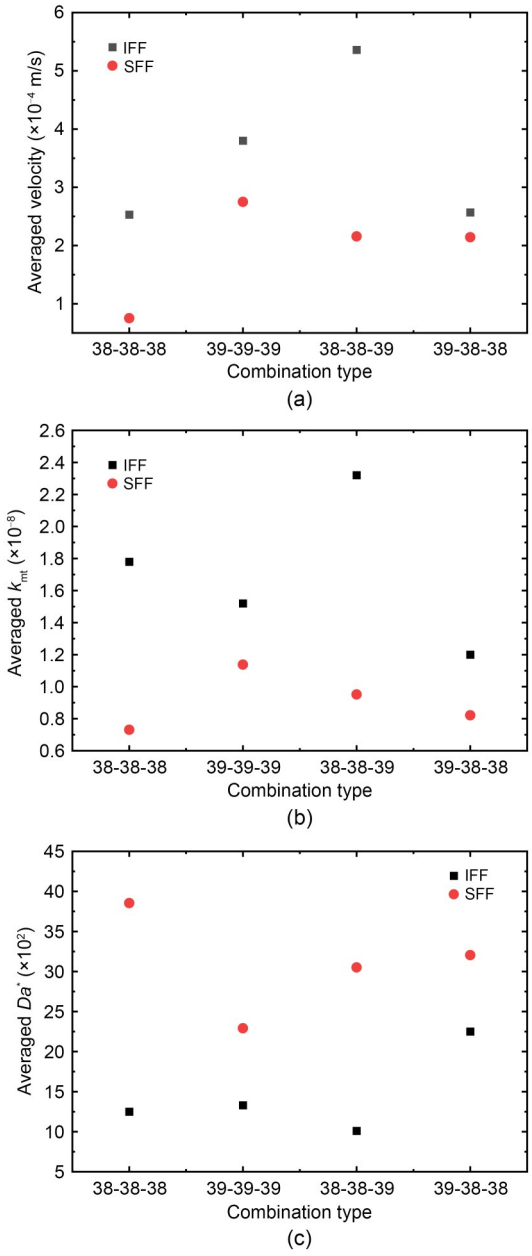


Fig. 7 (a) Averaged electrolyte flow velocity; (b) averaged effective mass transfer coefficient; (c) averaged Damköhler number in the three-layer CP electrode obtained through simulation. Testing was based on a flow rate of 5 mL/min

For the VRFB with the IFF, the 38-38-39 combination has the highest electrolyte flow velocity, the most efficient mass transfer coefficient, and the smallest Damköhler number. This finding aligns with the optimal polarization curve discussed in Section 3.1. Note that higher flow rates do not necessarily correspond to larger effective mass transfer coefficients. For instance, although the 39-39-39 combination has a higher velocity than the 38-38-38 combination, its effective mass transfer coefficient is lower. This is because the effective mass transfer coefficient is not solely dependent on velocity but is also affected by microscopic factors such as pore diameter and specific surface area. On the other hand, for the VRFB with the SFF, the 39-39-39 combination has the highest velocity and effective mass transfer coefficient, along with the smallest Damköhler number, which is consistent with the findings in Section 3.2. Meanwhile, due to the poor permeability of CP, the overall electrolyte flow velocity of the VRFB with the SFF is low, the effective mass transfer coefficient is small, and the Damköhler number is relatively large. Consequently, this leads to its overall subpar performance. In summary, the Damköhler number is directly correlated with the polarization performance of VRFBs. The heterogeneous design of porous electrodes effectively balances the relative rates of mass transfer and electrochemical reactions, thereby minimizing the Damköhler number and consequently improving VRFBs performance. This insight offers a more reliable theoretical foundation for future optimization of porous electrode structures.

4.2 Effects of the inlet flow rate

The polarization curve presented in Section 3 shows a pronounced drop, indicating that the related analysis is applicable exclusively to the mass transfer-limited regime. Considering the alterations in the inlet flow rate of the VRFB, which directly influence the electrolyte flow velocity within the porous electrode and the effective mass transfer coefficient in the diffusion layer, ultimately affecting Da^*, we experimentally examine the polarization curves of the VRFB with the IFF and SFF at higher flow rates and mass transfer-unlimited conditions. As shown in Figs. 8a and 8b, an increase in the inlet flow rate has a certain positive effect on both the IFF and SFF. However, the performance improvement of the VRFB using the IFF is more notable (the value of the critical current density nearly doubled). This is because the augmented inlet flow can be fully manifested as an enhanced electrolyte flow velocity in the porous electrode, ultimately reducing Da^*. For the SFF, although an increased flow rate can facilitate the penetration of the electrolyte into the electrodes, its impact is restricted. Additionally, when the flow rate is increased, the polarization

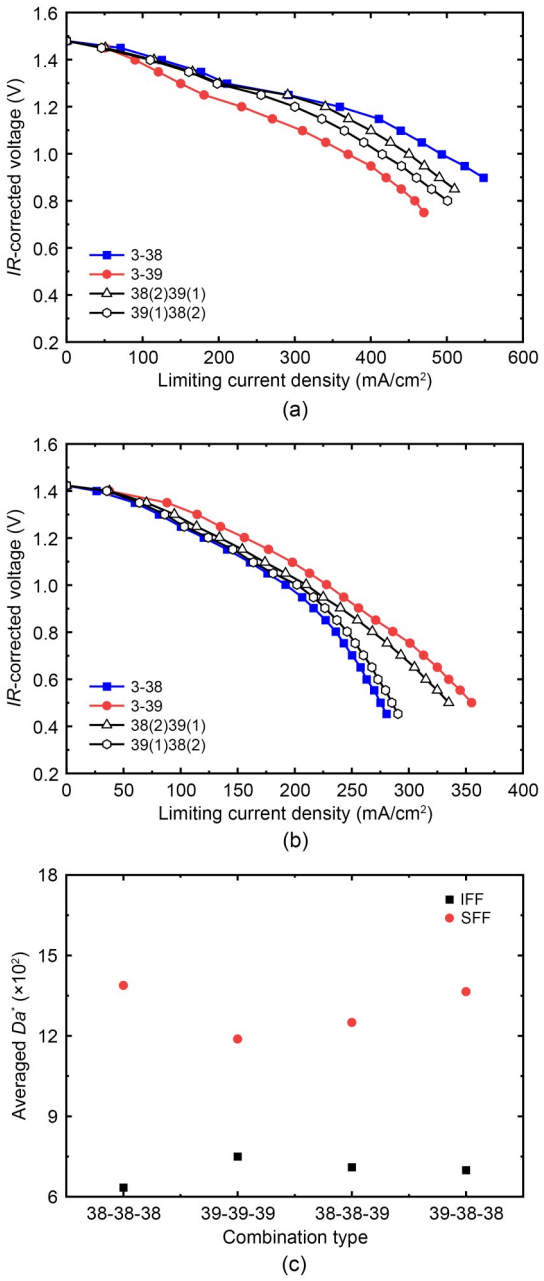


Fig. 8 *IR*-corrected polarization curves of the VRFB flow cell with (a) IFF and (b) SFF and (c) corresponding Damköhler numbers at an inlet flow rate of 20 mL/min

performance of the 38-38-38 combination for the VRFB with the IFF surpasses that of the 38-38-39 combination. This is because the flow rate within the porous electrode is sufficiently high at this stage to counteract the adverse effects of poor mass transfer near the membrane side, ultimately attaining the lowest Da^* value.

4.3 Effects of the types of electrodes

Given the significant differences between CP and graphite felt (GF) porous electrodes in terms of pore diameter, specific surface area, and permeability, we investigate their different effects on the IFF and SFF. The order of the channel and porous electrode combinations from highest to lowest performance is IFF-CP> SFF-GF>SFF-CP>IFF-GF. This order aligns with the corresponding Da^* trend. Note that, in general, the permeability of GF is one to two orders of magnitude higher than that of CP. When GF is used as the electrode material, the performance of the SFF is markedly superior to that of the IFF, further highlighting the significance of electrode permeability in SFF applications.

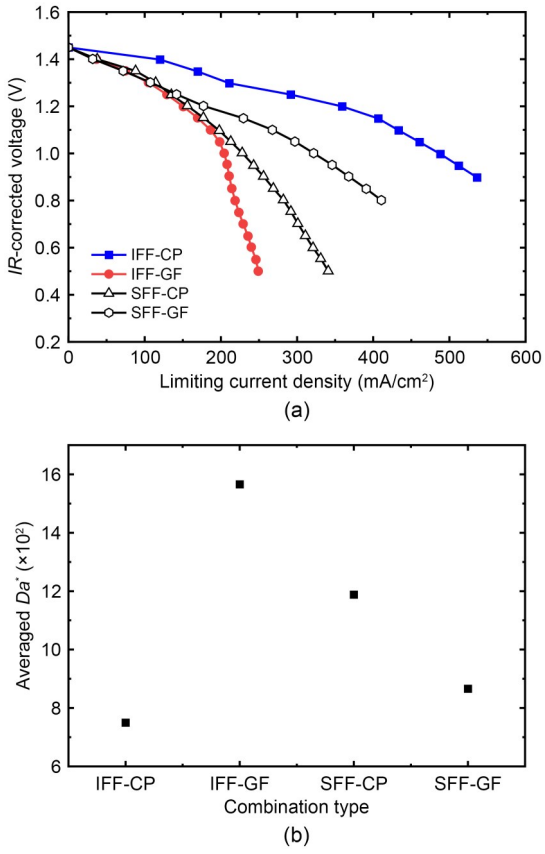


Fig. 9 (a) *IR*-corrected polarization curves of the VRFB flow cell with different flow fields and porous electrodes based on an inlet flow rate of 5 mL/min; (b) corresponding Damköhler numbers. The thickness of the different electrodes was maintained at the same magnitude

4.4 Future work

After a series of studies, we find that although heterogeneous electrode design has a significant effect on the IFF, its effect on the SFF is very small. In this context, we formulate preliminary concepts concerning the heterogeneous design of porous electrodes for the SFF. Given that the electrolyte flow within the SFF structure may induce concentration variations along the in-plane direction of the electrode, implementing a heterogeneous design along this axis can yield more substantial performance enhancements. Nevertheless, due to practical limitations in the fabrication of porous electrodes with such designs, this line of research has not yet been fully realized. Advanced manufacturing techniques, such as three-dimansional printing, may enable complex heterogeneous designs along the in-plane direction in the future.

5 Conclusions

We undertake a systematic and comprehensive study of the heterogeneous optimization of porous electrodes in VRFBs with different flow fields, using both experimental and simulation approaches. The main findings are as follows:

1. For VRFBs with the IFF, the heterogeneous design of porous electrodes has a notable influence. Owing to the poor mass transfer resulting from the low electrolyte flow velocity near the membrane side of the porous electrode, adopting a structure with a higher porosity at this location is often effective.

2. For VRFBs with the SFF, since the flow field fails to compel all the electrolyte to penetrate the porous electrode, ensuring the permeability of the porous electrode becomes the primary objective, aiming to guarantee the penetration flow rate and mass transfer efficiency of the electrolyte within the porous electrode. Nevertheless, the optimization design of heterogeneity has a limited impact.

3. Furthermore, the effectiveness of the porous electrode depends on a balanced relationship between the mass transfer rate of the reactants and the rate of the

electrochemical reaction. We introduce the Damköhler number to quantify this balance and serve as a basis for subsequent optimization. The validity of this parameter is verified under different combinations of channels and electrodes.

Acknowledgments

This work is supported by the Ningbo Natural Science Foundation of China (Nos. 2023J398 and 2023J276), the Zhejiang Provincial Natural Science Foundation of China (No. LQ23E060003), and the Fundamental Research Funds for the Central Universities (No. 2022ZFJH004), China.

Author contributions

Jie SUN and Menglian ZHENG designed the research. Jie SUN and Mengxin YU processed the corresponding data. Jie SUN wrote the first draft of the manuscript. Menglian ZHENG helped to organize the manuscript. Jianxin LI, Jinbo CHEN, and Changxing HU revised and edited the final version.

Conflict of interest

Jie SUN, Menglian ZHENG, Mengxin YU, Jinbo CHEN, Jianxin LI, and Changxing HU declare that they have no conflict of interest.

References

Alphonse PJ, Taş M, Elden G, 2023. Novel electrode design having gradually increasing porosity in a vanadium redox flow battery. *Fuel*, 333:126198. https://doi.org/10.1016/j.fuel.2022.126198

Chen W, Kang JL, Shu Q, et al., 2019. Analysis of storage capacity and energy conversion on the performance of gradient and double-layered porous electrode in all-vanadium redox flow batteries. *Energy*, 180:341-355. https://doi.org/10.1016/j.energy.2019.05.037

Duan ZN, Zhang GB, Zhang JF, et al., 2022. Experimental investigation on the performance characteristics of flow fields in redox flow batteries under various electrode parameters. *Frontiers in Thermal Engineering*, 2:931160. https://doi.org/10.3389/fther.2022.931160

Forner-Cuenca A, Brushett FR, 2019. Engineering porous electrodes for next-generation redox flow batteries: recent progress and opportunities. *Current Opinion in Electrochemistry*, 18:113-122. https://doi.org/10.1016/j.coelec.2019.11.002

Gautam RK, Kumar A, 2022. A review of bipolar plate materials and flow field designs in the all-vanadium redox flow battery. *Journal of Energy Storage*, 48:104003. https://doi.org/10.1016/j.est.2022.104003

He ZX, Lv YR, Zhang TA, et al., 2022. Electrode materials for vanadium redox flow batteries: intrinsic treatment and introducing catalyst. *Chemical Engineering Journal*, 427: 131680. https://doi.org/10.1016/j.cej.2021.131680

Houser J, Clement J, Pezeshki A, et al., 2016. Influence of architecture and material properties on vanadium redox flow battery performance. *Journal of Power Sources*, 302: 369-377. https://doi.org/10.1016/j.jpowsour.2015.09.095

Houser J, Pezeshki A, Clement JT, et al., 2017. Architecture for improved mass transport and system performance in redox flow batteries. *Journal of Power Sources*, 351:96-105. https://doi.org/10.1016/j.jpowsour.2017.03.083

Hu GJ, Jing MH, Wang DW, et al., 2018. A gradient bifunctional graphene-based modified electrode for vanadium redox flow batteries. *Energy Storage Materials*, 13:66-71. https://doi.org/10.1016/j.ensm.2017.12.026

Huang ZB, Mu AL, 2021. Flow field design and performance analysis of vanadium redox flow battery. *Ionics*, 27(12): 5207-5218. https://doi.org/10.1007/s11581-021-04213-8

Huang ZB, Mu AL, Wu LX, et al., 2022a. Comprehensive analysis of critical issues in all-vanadium redox flow battery. *ACS Sustainable Chemistry & Engineering*, 10(24): 7786-7810. https://doi.org/10.1021/acssuschemeng.2c01372

Huang ZB, Mu AL, Wu LX, et al., 2022b. Vanadium redox flow batteries: flow field design and flow rate optimization. *Journal of Energy Storage*, 45:103526. https://doi.org/10.1016/j.est.2021.103526

Huynh TTK, Yang T, Nayanthara PS, et al., 2025. Construction of high-performance membranes for vanadium redox flow batteries: challenges, development, and perspectives. *Nano-Micro Letters*, 17(1):260. https://doi.org/10.1007/s40820-025-01736-x

Jiang HR, Shyy W, Wu MC, et al., 2019a. A bi-porous graphite felt electrode with enhanced surface area and catalytic activity for vanadium redox flow batteries. *Applied Energy*, 233-234:105-113. https://doi.org/10.1016/j.apenergy.2018.10.033

Jiang HR, Zhang BW, Sun J, et al., 2019b. A gradient porous electrode with balanced transport properties and active surface areas for vanadium redox flow batteries. *Journal of Power Sources*, 440:227159. https://doi.org/10.1016/j.jpowsour.2019.227159

Lv WR, Luo YS, Xu YH, et al., 2024. Laser perforated porous electrodes in conjunction with interdigitated flow field for mass transfer enhancement in redox flow battery. *International Journal of Heat and Mass Transfer*, 224:125313. https://doi.org/10.1016/j.ijheatmasstransfer.2024.125313

Maurya S, Nguyen PT, Kim YS, et al., 2018. Effect of flow field geometry on operating current density, capacity and performance of vanadium redox flow battery. *Journal of Power Sources*, 404:20-27. https://doi.org/10.1016/j.jpowsour.2018.09.093

Mukhopadhyay A, Yang Y, Li YF, et al., 2019. Mass transfer and reaction kinetic enhanced electrode for high-performance aqueous flow batteries. *Advanced Functional Materials*,

29(43):1903192.
https://doi.org/10.1002/adfm.201903192

Muñoz-Perales V, García-Salaberri PÁ, Mularczyk A, et al., 2023. Investigating the coupled influence of flow fields and porous electrodes on redox flow battery performance. *Journal of Power Sources*, 586:233420.
https://doi.org/10.1016/j.jpowsour.2023.233420

Pezeshki AM, Sacci RL, Delnick FM, et al., 2017. Elucidating effects of cell architecture, electrode material, and solution composition on overpotentials in redox flow batteries. *Electrochimica Acta*, 229:261-270.
https://doi.org/10.1016/j.electacta.2017.01.056

Sun J, Zheng ML, Yang ZS, et al., 2019a. Flow field design pathways from lab-scale toward large-scale flow batteries. *Energy*, 173:637-646.
https://doi.org/10.1016/j.energy.2019.02.107

Sun J, Zheng ML, Luo YS, et al., 2019b. Three-dimensional detached serpentine flow field design for redox flow batteries. *Journal of Power Sources*, 428:136-145.
https://doi.org/10.1016/j.jpowsour.2019.04.106

Sun J, Liu BC, Zheng ML, et al., 2022. Serpentine flow field with changing rib width for enhancing electrolyte penetration uniformity in redox flow batteries. *Journal of Energy Storage*, 49:104135.
https://doi.org/10.1016/j.est.2022.104135

Sun J, Luo YS, Zheng ML, et al., 2023. An analytical model for parametric study on serpentine and interdigitated flow fields in redox flow batteries. *Journal of Energy Storage*, 71:108188.
https://doi.org/10.1016/j.est.2023.108188

Wan SB, Liang XW, Jiang HR, et al., 2021. A coupled machine learning and genetic algorithm approach to the design of porous electrodes for redox flow batteries. *Applied Energy*, 298:117177.
https://doi.org/10.1016/j.apenergy.2021.117177

Wang PF, Zhao YJ, Ban YH, et al., 2024. A review of porous electrode structural parameters and optimization for redox flow batteries. *Journal of Energy Storage*, 97:112859.
https://doi.org/10.1016/j.est.2024.112859

Wang YH, Li M, Hao L, 2022. Three-dimensional modeling study of all-vanadium redox flow batteries with the serpentine and interdigitated flow fields. *Journal of Electroanalytical Chemistry*, 918:116460.
https://doi.org/10.1016/j.jelechem.2022.116460

Ye JY, Zheng CH, Liu J, et al., 2022. In situ grown tungsten trioxide nanoparticles on graphene oxide nanosheet to regulate ion selectivity of membrane for high performance vanadium redox flow battery. *Advanced Functional Materials*, 32(8):2109427.
https://doi.org/10.1002/adfm.202109427

Ye JY, Xia L, Li HY, et al., 2024. The critical analysis of membranes toward sustainable and efficient vanadium redox flow batteries. *Advanced Materials*, 36(28):2402090.
https://doi.org/10.1002/adma.202402090

Ye LZ, Qi ST, Cheng TK, et al., 2024. Vanadium redox flow battery: review and perspective of 3D electrodes. *ACS Nano*, 18(29):18852-18869.
https://doi.org/10.1021/acsnano.4c06675

Yoon SJ, Kim S, Kim DK, 2019. Optimization of local porosity in the electrode as an advanced channel for all-vanadium redox flow battery. *Energy*, 172:26-35.
https://doi.org/10.1016/j.energy.2019.01.101

Zarei-Jelyani M, Loghavi MM, Babaiee M, et al., 2023. The significance of charge and discharge current densities in the performance of vanadium redox flow battery. *Electrochimica Acta*, 443:141922.
https://doi.org/10.1016/j.electacta.2023.141922

Zeng C, Kim S, Chen YX, et al., 2023. In situ characterization of kinetics, mass transfer, and active electrode surface area for vanadium redox flow batteries. *Journal of the Electrochemical Society*, 170(3):030507.
https://doi.org/10.1149/1945-7111/acbf7f

Zheng ML, Liu K, Sun J, et al., 2024. Quantifying effects of surface morphology and functional groups of carbon fibers on mass transfer coefficient in vanadium redox flow batteries. *Energy*, 291:130237.
https://doi.org/10.1016/j.energy.2024.130237

Electronic supplementary materials

Sections S1–S3, Table S1, Figs. S1 and S2